4-2 Overview of the Laser Communication System for the NICT Optical Ground Station and Laser Communication Experiments on Ground-to-Satellite Links

TOYOSHIMA Morio, KURI Toshiaki, KLAUS Werner, TOYODA Masahiro, TAKENAKA Hideki, SHOJI Yozo, TAKAYAMA Yoshihisa, KOYAMA Yoshisada, KUNIMORI Hiroo, JONO Takashi, YAMAKAWA Shiro, and ARAI Katsuyoshi

The National Institute of Information and Communications Technology (NICT) conducts research and development of laser communication technologies necessary for the realization and quality improvement of optical space communications. An in-orbit verification experiment of the inter-orbit optical communication link between the Optical Inter-orbit Communications Engineering Test Satellite (OICETS) (known as "Kirari"), which was developed by the Japan Aerospace Exploration Agency (JAXA), and the Advanced Relay Technology Mission Satellite (ARTEMIS), developed by the European Space Agency (ESA), was successfully conducted in December 2005. Kirari was launched by a Dnepr Launch Vehicle from the Baikonur Cosmodrome in the Republic of Kazakhstan and injected into Low Earth Orbit (LEO) at an altitude of 610 km and an inclination of 97.8°. The functionality of the satellite systems was checked during the first three months, in which acquisition and tracking of stars and planets was successfully performed. In December 2005, the first bidirectional laser communication link between Kirari and ARTEMIS was successfully established. The Kirari optical communication demonstration experiment with the NICT optical ground station (KODEN) was successfully realized because the optical antenna can be pointed toward the optical ground station with a special satellite attitude control system. The objectives of KODEN were to confirm the tracking abilities of Kirari and the optical ground station in the presence of atmospheric turbulence, as well as to verify the capabilities of laser communication systems with respect to ground-to-LEO satellite links. Phases 1, 2, and 3 of the bidirectional ground-to-satellite laser communication experiment were successfully performed in March, May, and September 2006, and Phase 4 of the experiment was conducted between October 2008 and February 2009 under research collaboration with JAXA. In this paper, the results obtained in Phases 1–4 of the KODEN experiment are summarized.

1 Introduction

The advantages of optical communication, as compared with radio frequency (RF) communication, include a wider bandwidth, a larger transfer capacity, lower power consumption, more compact equipment, greater security against eavesdropping and protection against interference [1][2]. As the demand for high data transmission rates from space-borne plat-

forms is steadily increasing [3], it is highly important to ensure steady operation of the on-board optical terminal and to complete numerous successful in-orbit demonstrations of optical space communication.

The Optical Inter-orbit Communications Engineering Test Satellite (OICETS) (known as "Kirari"), which was developed by the Japan Aerospace Exploration Agency (JAXA), was launched by the Dnepr Launch Vehicle from the Baikonur Cosmodrome in the Republic of Kazakhstan and injected into a low earth orbit (LEO) at an altitude of 610 km and an inclination of 97.8°. In December 2005, the first bidirectional laser communication link between Kirari and the Advanced Relay Technology Mission Satellite (ARTEMIS), developed by the European Space Agency (ESA), was successfully established [4]. The results of this experiment are reported in entries **3-1** and **3-2** in this special issue.

The satellite attitude of OICETS can be fixed in the inertia field at the far side of the ground station, and after half an orbital revolution the optical antenna onboard OICETS faces the optical ground station. Therefore, the experiment on optical communication between OICETS and the National Institute of Information and Communications Technology (NICT, formerly CRL) optical ground station located in Koganei, Tokyo, Japan, was conducted while the satellite was accessible from the ground station above an elevation angle of 15° [5]. Since in these experiments it was essential to suppress atmospheric turbulence, NICT developed a fine-steering mirror (to couple the downlink laser signal into a single-mode fiber [6]) as well as a real-time Low-Density Parity-Check (LDPC) decoder constructed from a field-Programmable Gate Array (FPGA) [7][8]. The verification experiment was conducted by using actual ground-to-satellite laser communication links (cf. parts **4-3** and **4-4** in this special issue). In this paper, an overview of the laser communication system at the NICT optical ground station and the results of the experiment are described.

2 History of laser-based space communication

2.1 Research on laser beam propagation to satellites

Extensive research on the theory of laser propagation in the presence of atmospheric turbulence has been conducted since the 1970s [9][10]. The first theoretical study on scintillation for an uplink laser transmission to a satellite was performed by Fried in 1967 [11]. Several years later, Minott discussed experimental data obtained in 1968 from a continuous-wave (CW) argon laser illuminating the Geodetic Earth Orbiting Satellite II (GEOS-II) [12]. In 1973, in a study similar to that conducted by Fried, Titterton examined focused and defocused beams and concluded that on-axis scintillation can be reduced even further with a focused beam [13][14]. Fried also considered the effect of pointing jitter on the probability distribution for the strength of the received signal and showed that the log intensity takes the particularly simple form of an exponential distribution [15]. Measurements of scintillation on a vertical path from a ground-based laser transmitter to the GEOS-III satellite and back to the transmitter were reported by Bufton in 1977 and compared with the theoretical model [16].

In 1983, Yura and McKinley published a theoretical study on fades and surges for a ground-to-space link in which the transmitted wave is a spherical wave operating in the 1–10 μm wavelength regime [17]. In the Relay Mirror Experiment (RME) conducted by the Strategic Defense Initiative Organization (SDIO) in the early 1990s, three laser beams were projected from two ground sites at the Air Force Maui Optical Station (AMOS) in Hawaii, US. These beams were both retroreflected and reflected from the RME satellite orbiting at an altitude of 350 km. The uplink beam intensity profile at the satellite appeared as a moderately distorted form of an idealized Gaussian beam profile [18]. In 1994, Kiasaleh derived expressions for the probability density function (PDF) of the optical signal intensity in an opti-

cal communication channel and investigated the impact of the residual pointing error caused by imperfect tracking for various channel scattering models as a result of the Galileo Optical Experiment (GOPEX) [19]. In 1995, Shelton published expressions describing the variance and the power spectral density of turbulence-induced log-amplitude fluctuations associated with an uplink Gaussian beam wave with the Low-Power Atmospheric Compensation Experiment (LACE) satellite developed by the US Naval Research Laboratory [20].

In 1995, Andrews et al. derived estimates for the beam spot size, scintillation index, fractional fade time, expected number of fades and mean duration of the fade time associated with both the uplink and the downlink propagation channels for a laser satellite communication system [21]. In 2000, Andrews et al. extended their scintillation model for a satellite communication link from the moderate- to the strong-turbulence regime. This scintillation model was derived as a modulation process in which the small-scale (diffractive) fluctuation was multiplicatively modulated by the large-scale (refractive) fluctuation. The results agreed well with the conventional weak scintillation theory for zenith angles of less than 45-60°. The PDF for the moderate-to-strong-turbulence regime was described sufficiently well by the gamma-gamma distribution, which was also in close agreement with simulation data [22]-[24].

2.2 Laser beam transmission experiments at NICT

NICT has been researching horizontal laser beam propagation since the 1970s [25][26]. An experiment on laser beam transmission from the ground to the Engineering Test Satellite Ⅲ (ETS-Ⅲ) was conducted by using a camera onboard the satellite [27], followed by an experiment on laser transmission to Geostationary Meteorological Satellite (GMS) at wavelengths of 0.5 μm and 10.6 μm [28][29]. Another experiment focused on position correction using the uplink laser beam transmission with the Marine Observation Satellite-1b

(MOS-1b) [30]. In 1989, the space optical communication ground station was developed [31], and the satellite laser ranging (SLR) experiment was performed with geodesic satellites (Ajisai, LAGEOS). An experiments involving SLR to the Retro-reflector In-Space (RIS) onboard the ADEOS satellite was conducted by using a CO_2 laser radar, and a similar experiment was conducted by using the Laser Reflecting Equipment (LRE) onboard a H-ⅡA launch vehicle [34][35]. Between 1994 and 1996, the first ground-to-geostationary satellite laser communication experiments were successfully conducted by using the Laser Communication Equipment (LCE) onboard the Engineering Test Satellite Ⅵ (ETS-Ⅵ) [36] [37]. In 2004, an experiment on laser transmission to a CMOS camera onboard the Microlabsat 1 (μ-LabSat) was successfully performed [38][39]. After the KODEN experiment, NICT is currently planning in-orbit laser communication experiments with 50-kg class microsatellites [40], and it is important to verify the tracking and pointing performance of the NICT optical ground station by using LEO satellites.

2.3 First ground-to-LEO laser communication experiment

In Japan, NICT successfully performed the first bidirectional laser communication demonstration using the laser communication equipment onboard the ETS-Ⅵ satellite in Geosynchronous Earth Orbit (GEO) [36], and a ground-to-ARTEMIS optical communication experiment using the Semiconductor Intersatellite Laser EXperiment (SILEX) optical terminal was successfully conducted in collaboration with the ESA optical ground station in Tenerife, Spain [41]. However, with low earth orbit (LEO) satellites, acquiring and tracking the counter terminal is particularly difficult due to the high angular velocity of such satellites. In the Relay Mirror Experiment (RME) in the early 1990s, three laser beams were projected from two ground sites in Hawaii. These beams were both retroreflected and reflected from the RME satellite orbiting at 350 km.

The uplink beam intensity profile was measured, however, there was no laser communication experiment [18]. Furthermore, the Ballistic Missile Defense Organization (BMDO) developed laser communication terminal equipment for the BMDO Space Technology Research Vehicle 2 experiment. Unfortunately, the experiment ended in failure in 2000 due to a large attitude error in the host satellite [42]. Therefore, to our knowledge, KODEN was the first in-orbit optical communication demonstration using a LEO satellite.

3 Overview of the experiment

3.1 Configuration of the experimentation system

Phases 1, 2 and 3 of the bidirectional ground-to-satellite laser communication experiment, named KODEN, were successfully performed in March, May and September 2006, and Phase 4 was conducted between October 2008 and February 2009. This experiment was conducted in cooperation with JAXA. Figure 1 shows the configuration of the KODEN experiment. The onboard optical antenna (a center-feed Cassegrain mirror-type telescope with a diameter of 26 cm attached to the -Z-axis panel) usually faces away from Earth for experiments on inter-orbit communication with the GEO satellite ARTEMIS. For the experiment on communication with the optical ground station, the satellite attitude was fixed in the inertia field at the far side of the ground station, and after half an orbital revolu-
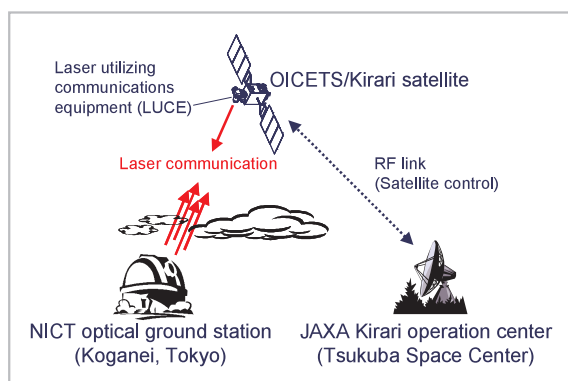

Laser utilizing communications equipment (LUCE)
OICETS/Kirari satellite

Laser communication

RF link
(Satellite control)

NICT optical ground station
(Koganei, Tokyo)

JAXA Kirari operation center
(Tsukuba Space Center)

Fig.1 Configuration of the ground-to-satellite laser communication experiment

tion the optical antenna onboard OICETS faced the optical ground station. The satellite was controlled from the JAXA Kirari operation center in Tsukuba, Ibaraki, Japan. The experiment on optical communication between OICETS and the NICT optical ground station was conducted while the satellite was accessible from the ground station above an elevation angle of 15°.

3.2 Objective of the experiment

The objective of the KODEN experiment was to evaluate the acquisition and tracking performance of the onboard LUCE terminal and the NICT optical ground station. The goals of the experiment with regard to the optical ground station are listed below:
(1) Verification of the establishment and maintenance of ground-to-LEO laser communication links.
(2) Improvement of tracking accuracy by using onboard Corner Cube Reflectors (CCRs).
(3) Acquisition of data on laser beam propagation and verification of the effects of atmospheric turbulence.

On the other hand, the goals with regard to the satellite included the following:
(1) Evaluation of the tracking characteristics at higher slew rates since this has been impossible to perform in the configuration used for inter-orbit experiments.
(2) Evaluation of the accuracy and stability of attitude control of the satellite.
(3) Improvement of the accuracy of determination of the satellite orbit.
(4) More efficient utilization of the satellite.
(5) Improving the capability of the satellite to provide massive data download rates.

As mentioned above, the direct downlink capability of LEO can be demonstrated with consideration for future communication requirements by verifying the ground-to-LEO laser communication with the laser communication terminal designed for GEO.

4 NICT optical ground station system

4.1 Configuration of NICT optical ground station

The fidelity of free-space laser communication between ground and satellite optical systems is degraded by the turbulent atmosphere of Earth. Possible techniques for compensating for the effects of scintillation include the use multibeam laser transmission [44] and adaptive optical systems [45]. However, adaptive optical systems cannot be easily applied to a link between a ground-based station and an LEO satellite due to the point-ahead angle. For this reason, the NICT optical ground station uses a multi-beam laser transmission system for the uplink, where laser beams are formed with different incoherent laser sources or the same laser source is divided into multiple beams with appropriate optical delays which correspond to the coherence length of the laser source [46]. A 1.5-m telescope is used for uplink transmission, and the sub-aperture of the 1.5-m telescope is used for downlink reception. The specifications of the optical signals are shown in Table 1.

4.2 Transmitter

Figure 2 shows a block diagram of the laser transmitter at the ground station. Two laser sources were used in the experiment, namely, a beacon beam with a broad divergence angle and a communication beam with a narrow divergence angle. The optical elements for the beacon beam were mounted beside the 1.5-m telescope tube. The divergence angle of the single uplink beacon beam in this system was 9 mrad, and its wavelength was 808 nm. This divergence angle was capable of covering the open pointing error of the optical ground station due to the prediction error of the satellite orbit. The beacon beam was fed into a multimode fiber with a core diameter of 400 μm, with a maximum power of 30 W, after which it was transmitted as shown in Fig. 3. Figures 4 and 5 show the beam profile and the phase of the beacon laser beam, respectively. The phase error was 0.150 λ (rms).

The optical elements for the communication beam were placed on a coude bench as shown in Fig. 6. The communication beam was transmitted from the laser source through the coude optical path and out the 1.5-m telescope by using open pointing control. A semiconductor laser beam with a wavelength of 815 nm and a maximum modulated output

Table 1   *Specifications of optical beams*

Parameter	Uplink		Downlink
	Beacon	Communication	
Wavelength	808 nm	815 nm	847 nm
Beam divergence angle (after 2008)	9 mrad	204 μrad (168 μrad)	5.5 μrad
Beam size	17 mmϕ	710 mmϕ	120 mmϕ
Transmitted power (at telescope aperture)	30 W (max)	10 mW	53 mW
Signal format	CW	2PPM	NRZ
Data rate	—	2.048 Mbps	49.3724 Mbps
Polarization	Random	LHCP, Random	LHCP
Number of beams	1	4	1
Receiving aperture diameter (March)	26 cmϕ	26 cmϕ	20 cmϕ
Receiving aperture diameter (after May 2006)	26 cmϕ	26 cmϕ	31.8 cmϕ (sub-aperture of the 1.5-m telescope)

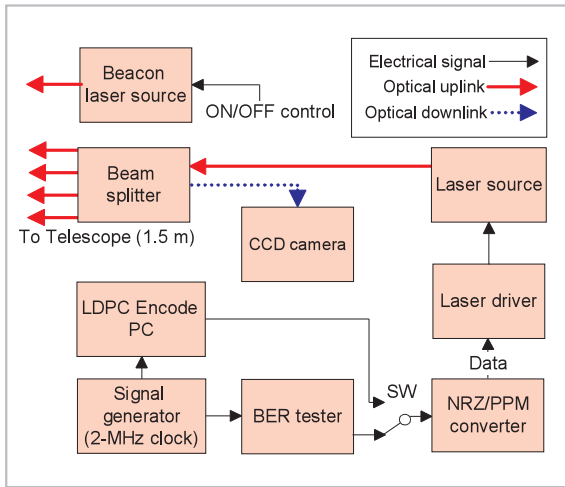Notes: 2PPM: 2-pulse position modulation, NRZ: non-return to zero, LHCP: left-hand circular polarization
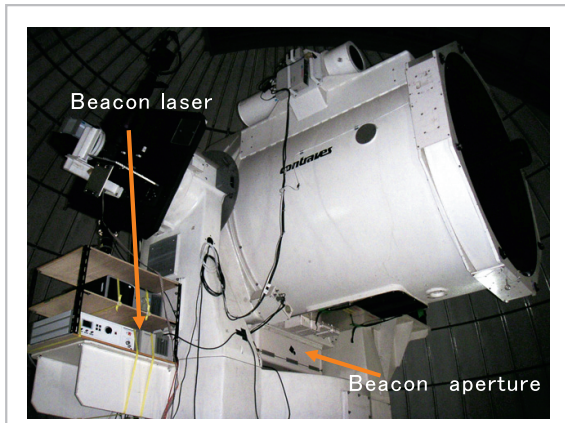
Fig.2 *Configuration of the transmitter*

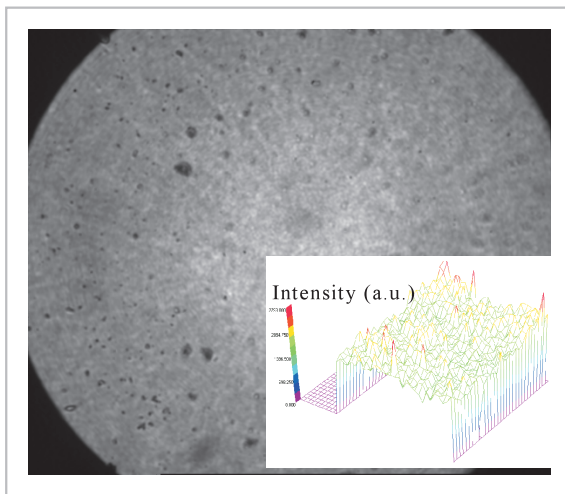**Fig.3** *The 1.5-m telescope, the beacon laser source and the beacon aperture*
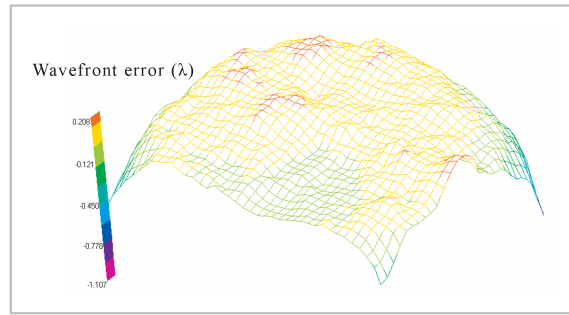

Fig.4 *Intensity profile of the beacon beam*

Fig.5 *Wavefront error of the beacon beam*

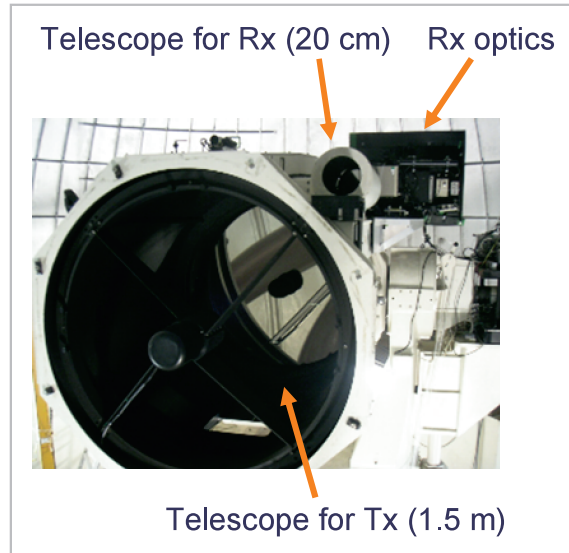Telescope for Rx (20 cm)   Rx optics

Telescope for Tx (1.5 m)

Fig.6 *The 1.5-m telescope for the transmitter and the 20-cm telescope for the receiver at the NICT optical ground station*

power of 500 mW was used with a multimode fiber with a core diameter of 100 μm. The intensity of the optical communication signal was modulated by the drive current at 2.048 Mbps. Furthermore, the uplink communication beam was divided into four parallel beams to reduce the effects of signal fluctuation caused by atmospheric turbulence (Fig. 7). Two bulk optical devices were used to generate four beams with appropriate optical delays, after which the beams were transmitted from the 1.5-m telescope, and the diameter of each beam at the 1.5 m primary telescope was 71.2 cm. The divergence angle of the uplink communication beam was 168 μrad, which was sufficient to cover the point-ahead angle of the satellite. The PDFs for various numbers of beams are shown in Fig. 8 for a scintillation
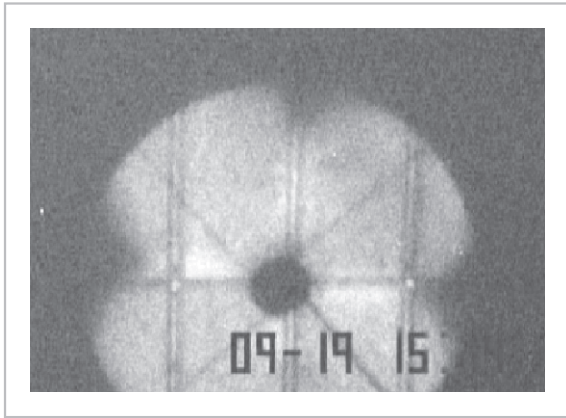
Fig.7   *Transmitted communication beam pattern consisting of four laser beams illuminating the dome wall*

Intensity (a.u.)

Fig.9   *Intensity profile of the communication beam*

Wavefront error (λ)

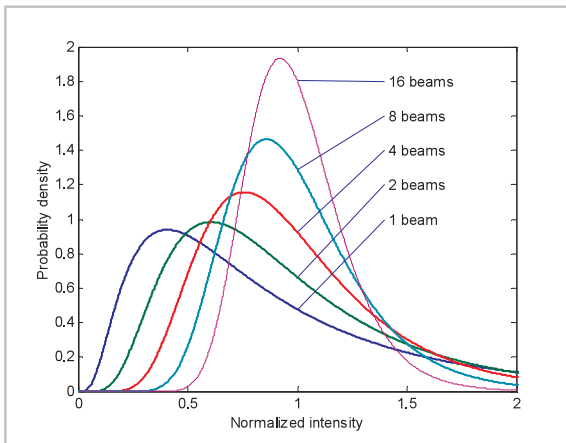**Fig.10**   *Wavefront error of the communication beam*

Fig.8   *Probability density function (PDF) of the received signal intensity, showing an improvement in variance with multiple uplink beams*

index of 0.6., where the average level and the probability level at low intensities increase with the number of beams. Figures 9 and 10 show the beam profile and the wavefront error of the transmitted communication beam. The wavefront error of the communication beam was 0.10 λ (Fig. 9).

4.3 Transmitter

In the experiment in 2006, an optical receiver was installed in a 20-cm telescope parallel to a 1.5-m telescope as shown in Fig. 6. After 2008, the optical receiver was located on the same coude bench as the transmitter optics. The configuration of the receiver is shown in Fig. 11, where the sub-aperture of the 1.5-m
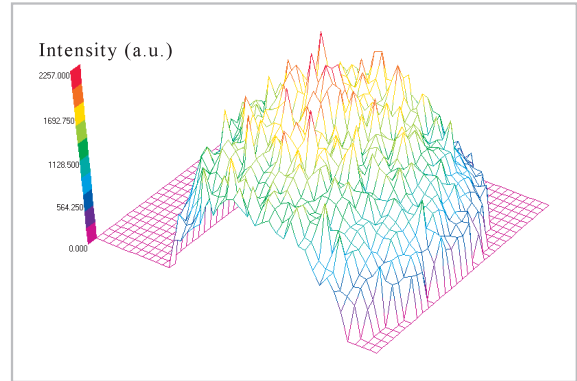
telescope was used for the coude optical path. Furthermore, the laser beam from OICETS was detected with a CCD camera, detectors with different apertures, a quadrant detector (QD) sensor and an avalanche photo detector (APD) receiver. The communication signal was detected with an APD receiver, and the bit error ratio (BER) was measured with a BER tester. The 50-Mbps data stream was simultaneously stored directly on a personal computer through a serial/parallel converter. It was necessary to receive –46 dBm of optical power to obtain a BER of 10^{-6}, as shown in Fig. 12. Since the sensitivity of the APD receiver was –48.4 dBm, this amounted to a difference of 2.4 dB.

In Phase 4 of the experiment, a real-time LDPC decoder was developed by using an FPGA. Three different codes were prepared with a length of 912 bits each due to hardware resource limitations of the FPGA, and two
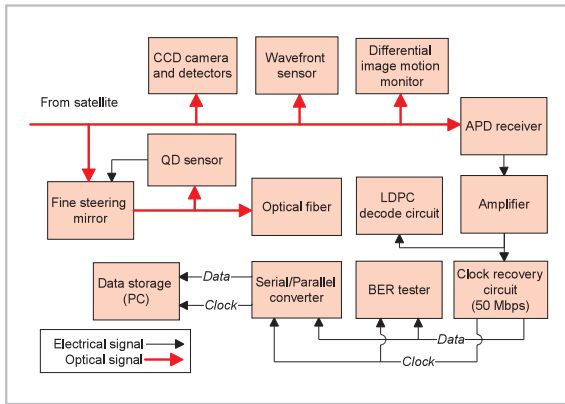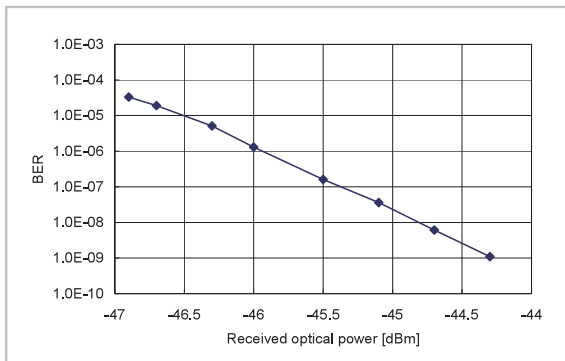
Table 2 Specifications of the DIMM system

Parameter	Value
Telescope aperture diameter	20 cm (March 2006) 1.5 m (after May 2006)
Magnification	10 (March 2006) 15.9 (after May 2006)
Diameter of subapertures	3.0 cm (March 2006) 4.8 cm (after May 2006)
Distance between subapertures	9.0 cm (March 2006) 14.3 cm (after May 2006)
Number of subapertures	4
Wedge angle	1°
ICCD sensor	Hamamatsu C5909-12
Exposure time	0.3 ms
CCD image pixels	768 × 494
Grabbed image pixels	640 × 480
Measured frame rate	30 fps

types of the prepared LDPC codes with different code lengths and coding rates were transmitted via the laser link in December 2008 and January 2009 (please refer to part **4-4** in this special issue). In addition, a new fine-steering mirror was developed, where piezoelectric actuators were used for the angular deflection of the attached mirror and a pre-load was applied to decrease the hysteresis effect. The frequency response was beyond 2 kHz, which was sufficient to compensate for the fluctuation in the rapidly moving angle of arrival caused by atmospheric turbulence (cf. paper **4-3** in this special issue).

4.4 Atmospheric turbulence measurements by the DIMM method

The Differential Image Motion Monitor (DIMM) method was used to estimate the atmospheric coherence length, and hence the seeing angle, of the ground-to-satellite optical link [47]. In DIMM measurements, four beam
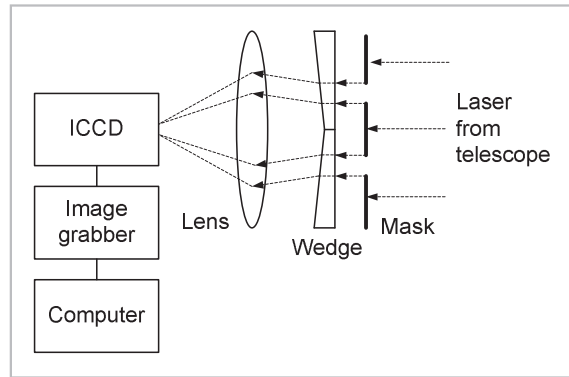
spots are formed on the CCD sensor. The DIMM measurement system is shown in Fig. 13, and its specifications are listed in Table 2. The two DIMM experiments were conducted with different optical setups. In March 2006, a 20-cm telescope was used for the DIMM measurement. After May 2006, the sub-aperture of the 1.5-m telescope fed into the coude path was used. A CCD camera with an image intensifier was used for the measurements. The merit of the differential image measurement method is that it protects the telescope from the effects of vibrational noise and the track-

ing error of the satellite.

4.5 Laser safety management

The total power of the communication laser beams transmitted from the aperture of the primary telescope at the optical ground station was about 10 mW (modulated), which conformed with safety regulations. In the operation of the optical ground station, laser beam transmission was permitted only at elevation angles of the telescope above 15° for safety reasons. Aircraft radar and observers to look out for airborne objects were employed to avoid interference. In addition, relevant information was announced to the police and the fire department when the experiments were executed.

5 Experimental results

5.1 Link statistics at the NICT optical ground station

Phases 1, 2, and 3 of the ground-to-satellite laser communication experiment were conducted in March, May, and September 2006, and Phase 4 was conducted between October 2008 and February 2009, after midnight, typically around 1:00-2:00 AM. The experimental results are shown in Tables 3(a) and 3(b) As shown in Fig. 14, the probability of success with respect to the acquisition and tracking of the satellite was 56% for the total number of test days assigned to Phases 1 through 4, and the experiment was always successful when partly clear or clear skies predominated.

The atmospheric transmission loss was estimated from the measured uplink and downlink received powers, as shown in Figs. 15 and 16, which show the cumulative probabilities of atmospheric attenuation as estimated from the uplink and downlink received powers. The results indicate that the optical ground station can access the satellite with a probability of 56% (Fig. 15), and the average atmospheric attenuation was estimated to be about 4.5 dB at 50% probability in the case of clear skies (Fig. 16). These are useful statistical data for atmospheric transmissions at the NICT optical ground station site over the course of one year.

5.2 Satellite acquisition

Figure 17 shows the laser beam from the

Table 3(a)	Summary of Phases 1–3 of the ground-to-OICETS satellite optical link experiment		
Test date	Session No.	Link established	Weather conditions
March 21, 2006	1	Yes	Clear
March 23, 2006	2	No	Cloudy
March 28, 2006	3	Yes	Clear
March 30, 2006	4	Yes	Partly cloudy
May 9, 2006	5	No	Rainy
May 11, 2006	6	Yes	Partly cloudy
May 16, 2006	7	Yes	Cloudy
May 18, 2006	8	No	Rainy
May 23, 2006	9	Yes	Partly cloudy
May 25, 2006	10	Yes	Partly cloudy
September 5, 2006	11	Yes	Clear
September 7, 2006	12	Yes	Partly cloudy
September 12, 2006	13	No	Rainy
September14, 2006	14	No	Cloudy
September 19, 2006	15	Yes	Clear
September 21, 2006	16	Yes	Partly cloudy
September 26, 2006	17	No	Rainy
September 28, 2006	18	No	Cloudy

| Test date	Session No.	Link established	Weather
October 16, 2008	1	No	Clear
October 21, 2008	2	Yes	Clear
October 23, 2008	3	No	Cloudy
October 28, 2008	4	Yes	Cloudy
October 30, 2008	5	No	Cloudy
November 4, 2008	6	No	Clear
November 6, 2008	7	No	Cloudy
November 11, 2008	8	No	Partly cloudy
November 13, 2008	9	Yes	Clear
November 18, 2008	10	Yes	Clear
November 20, 2008	11	Yes	Clear
November 25, 2008	12	No	Cloudy
November 27, 2008	13	No	Rainy
December 2, 2008	14	Yes	Clear
December 4, 2008	15	Yes	Thin clouds
December 9, 2008	16	No	Rainy
December 11, 2008	17	Yes	Clear
December 16, 2008	18	Yes	Partly cloudy
December 18, 2008	19	Yes	Clear
December 23, 2008	20	Yes	Clear
December 25, 2008	21	Yes	Clear
January 8, 2009	22	No	Rainy
January 13, 2009	23	Yes	Clear
January 15, 2009	24	Yes	Clear
January 20, 2009	25	Yes	Partly cloudy
January 29, 2009	26	No	Cloudy
February 10, 2009	27	No	Clear
February 24, 2009	28	No	Cloudy
February 26, 2009	29	No	Rainy
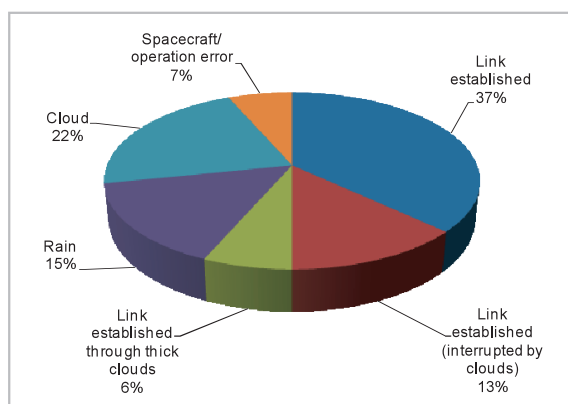
Fig.14 *Link establishment and associated weather conditions*
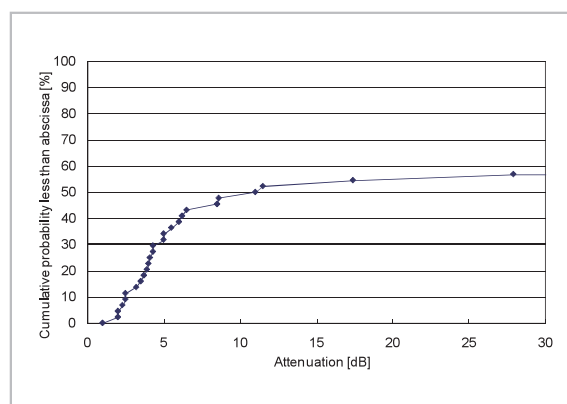

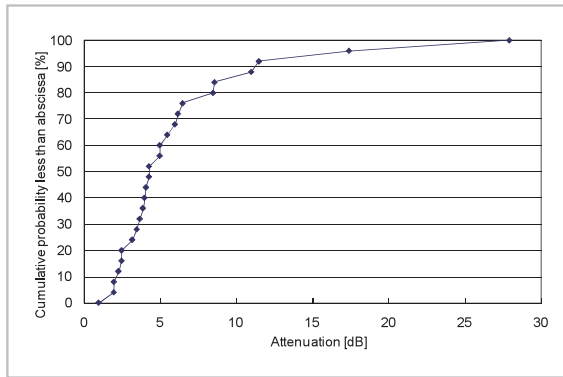**Fig.15** *Cumulative probability of atmospheric attenuation for all trials*

Fig.16 Cumulative probability of atmospheric attenuation for all trials where an optical link was established
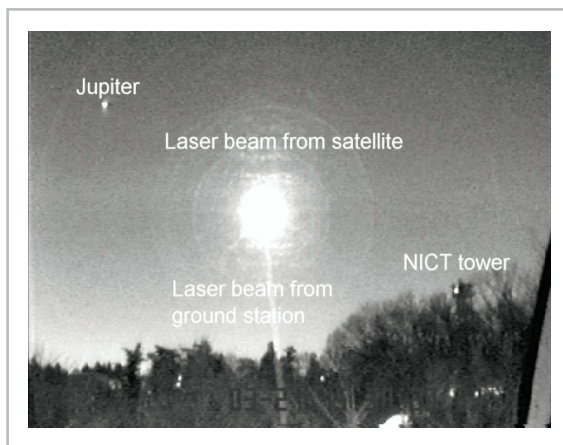
Fig.17 Laser beam from the LUCE terminal on-board OICETS (bright spot in the center) captured with a CCD video camera installed next to the 1.5-m telescope

Fig.18(a) Initial open pointing errors in Phases 1–3
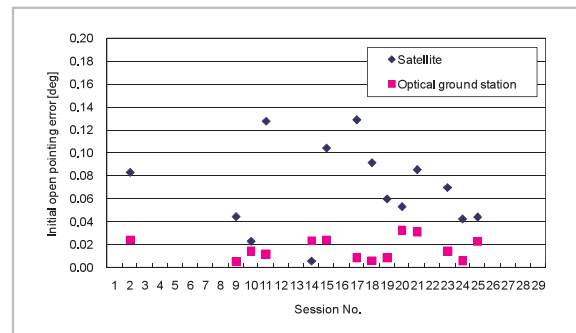
Fig.18(b) Initial open pointing errors in Phase 4

LUCE terminal onboard OICETS (bright spot in the center) as captured with a CCD video camera installed next to the 1.5-m telescope. Light scattered from the beacon laser beam transmitted from the ground station can be seen below the laser beam. Laser tracking was maintained across a cloudy sky. Both the beacon and communication beams were initially transmitted from the optical ground station, and the bias pointing error was eliminated by entering offset commands for the telescope. Once the telescope was optically aligned, the beacon beam was turned off with a shutter, which required 10-20 s, after which only modulated communication beams were transmitted. The beam divergence of the LUCE terminal was about 6 µrad. Therefore, the ground
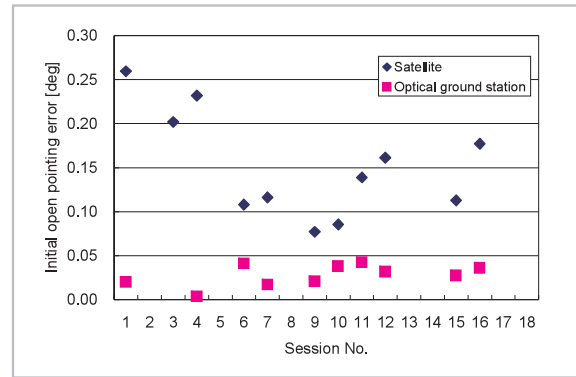
footprint of the beam from the satellite was only 6 m at a link distance of 1,000 km, as can be seen in Fig. 17.

5.3 Initial open pointing error

The initial open pointing errors of the on-board LUCE terminal and the NICT optical ground station are shown in Figs. 18(a) and 18(b), respectively. In Phases 1–3, the maximum initial open pointing error of the LUCE terminal was 0.259° in the first trial. The accuracy of the onboard satellite time was improved by JAXA, in which the error was reduced to a minimum of 0.08° and an average of 0.152° (2.65 mrad). The specified error for the onboard optical terminal was ±0.2°, and therefore the initial errors were within the specifications, except for the first three trials. In Phase 4, the maximum initial open pointing error of the LUCE terminal was less than 0.13° and the average open pointing error was 0.069° (= 1.2 mrad). The average open pointing error of the optical ground station was 0.017°
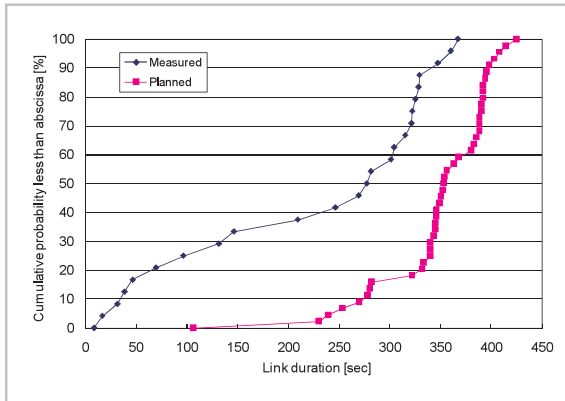
Fig.19 Cumulative probability of link duration

Fig.20 Tracking error along (a) the X axis and (b) the Y axis for the LUCE terminal (March 30, 2006)
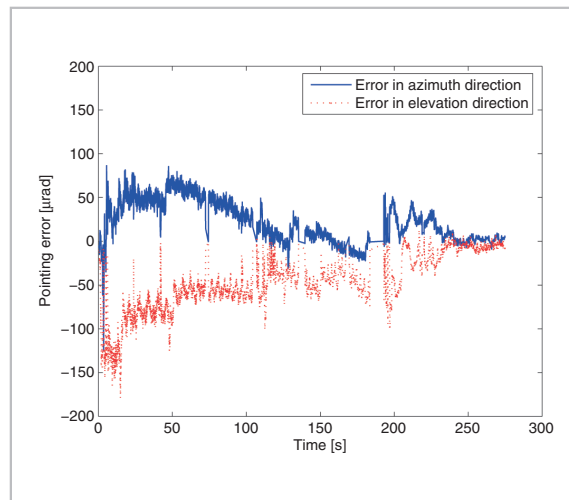
Fig.21 Telescope pointing errors (March 30, 2006)

(= 0.293 mrad), and it was mostly due to the ephemeris of OICETS. Since the divergence angle of the beacon beam was wide at 9 mrad (= 0.5°), it covered the open pointing error of the optical ground station. Figure 19 shows the cumulative probability of the link duration when tracking was successful. The planned cumulative probability was estimated by assuming clear skies for all experimental trials, and the measured probability represents the cumulative probability when the optical link was continuously connected in the experiment. The maximum link duration was 367 s in the experiment, which continued throughout the visible satellite pass above an elevation angle of 15° as seen from the NICT optical ground station. The average link duration was about 277 s due to interruptions caused by clouds, and it corresponds to about 78% of the average planned experiment time of 353 s.

5.4 Tracking and pointing errors

Figure 20 shows the fine tracking errors of the LUCE terminal onboard OICETS for a single trial. The errors during a complete pass were 0.67 and 1.47 µrad (rms) for the X and Y axes, respectively, and the total error was calculated to be 2.0 µrad (rss). Furthermore, the exact tracking direction is the direction corresponding to the center of the fine tracking sensor added to the residual tracking error of the fine tracking system. The exact total pointing direction includes the exact tracking direction and the point-ahead angle.
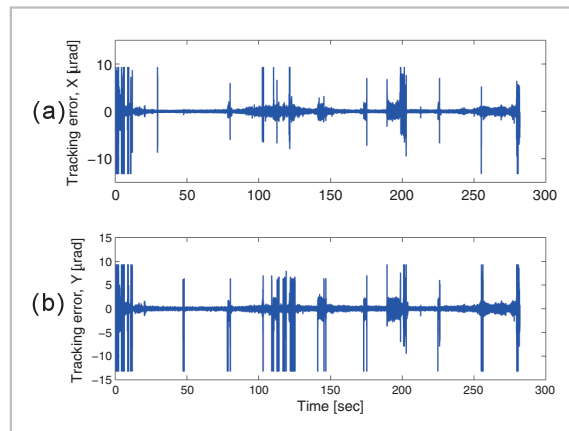
Figure 21 shows the telescope pointing errors of the ground station for a single trial. As the laser beams were transmitted using open pointing control, the errors during a complete pass were 23.8 and 32.7 µrad (rms) for the azimuth and elevation angles, respectively, and the total pointing error was 45.9 µrad (rss). Although the point-ahead angle varied (typically up to 50 µrad) during a single pass, the optical communication link was maintained without the use of point-ahead angle control at the ground station. In this regard, the pointing error of the uplink laser beams was well within the beam divergence angle.

5.5 Uplink and downlink laser transmission results

Figure 22 shows a plot of the uplink and downlink received power levels on September 19, 2006. As there was no average power control for either the uplink or the downlink, the received power varied with the propagation distance. Detection of the beacon laser beam was performed in the first 20 s and subsequently four laser beams were transmitted to OICETS. To evaluate the effect of multibeam transmission on the signal fluctuation, at around 200 s after detection, the number of laser beams was changed from 4 to 1 and increased accordingly afterward. In the downlink transmission, the received power was
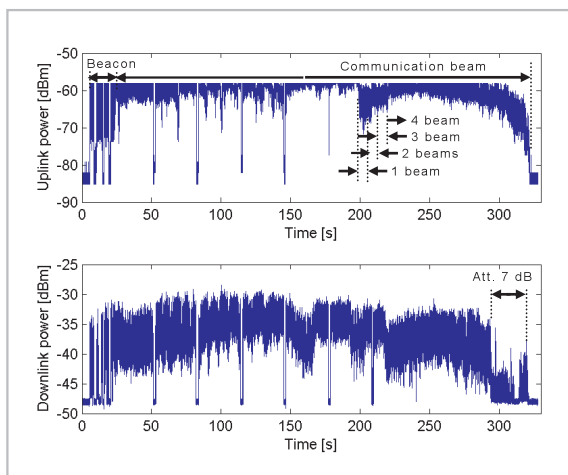
attenuated by 7 dB for the purpose of testing the optical receiver at the end of the experiment. The ground-to-OICETS optical link lasted for 321 s in this session. The received power showed some discontinuities caused by the operation of the coarse pointing system, resulting from the fast movement of the optical antenna onboard OICETS [47].

Figure 23 shows the PDF of the normalized intensity as a function of the number of laser beams with 1, 2, 3, and 4 laser beams at an elevation angle of around 35°. The signal variance decreased as the number of beams was increased. Figure 23 also shows the theoretically calculated lognormal distribution with a scintillation index of 0.14. The multibeam PDFs were calculated, showing close agreement between theoretical and measured data, excluding the saturated portion.

Figure 24 shows the scintillation indices for the uplink and downlink received signals as measured on September 19, 2006. The scintillation index is the normalized variance and is used as a measure for the level of atmospheric turbulence. The scintillation index is zero when there is no variation in the signal and above one in the case of strong atmospheric turbulence [48]. For the first 20 s, the scintillation index was around 0.6 for the uplink beacon laser beam at elevation angles above 15°. With four uplink laser beams, the
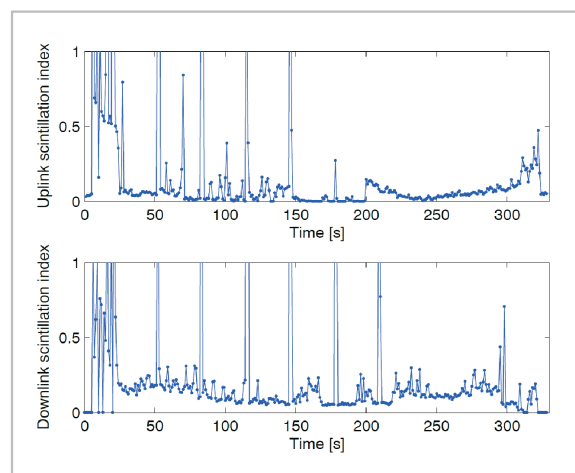

Fig.22 *Uplink and downlink received optical power measured on September 19, 2006*
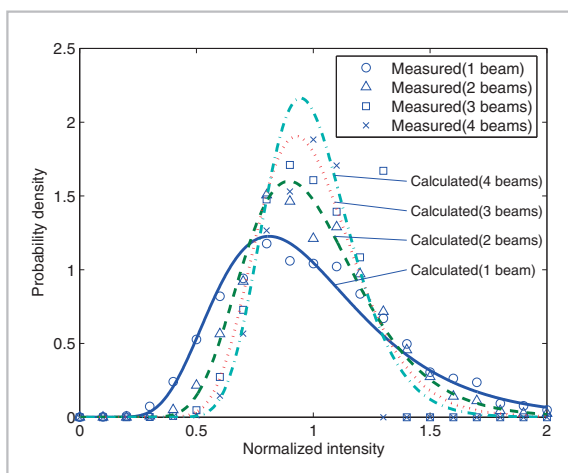
Fig.23 *Comparison between measured and calculated PDFs with a scintillation index of 0.14 from a single beam*

Fig.24 *Scintillation indices for the uplink and downlink received optical signals measured on September 19, 2006*

scintillation index was low throughout the experiment session because of the reduced effect of turbulence owing to the presence of multiple beams. The saturation of the optical sensor in the onboard optical terminal was observed (Fig. 23). For the downlink, since an aperture diameter of 31.8 cm was used in the optical ground station, the aperture averaging effect led to a reduction in turbulence-induced scintillation to around 0.2~0.3 (Fig. 23) [49][50].

Figures 25 and 26 show the long-term trends of the uplink and downlink received powers and the frequency spectra measured on March 28, 2006, where the abscissa shows the elapsed time during the experiment. The up-
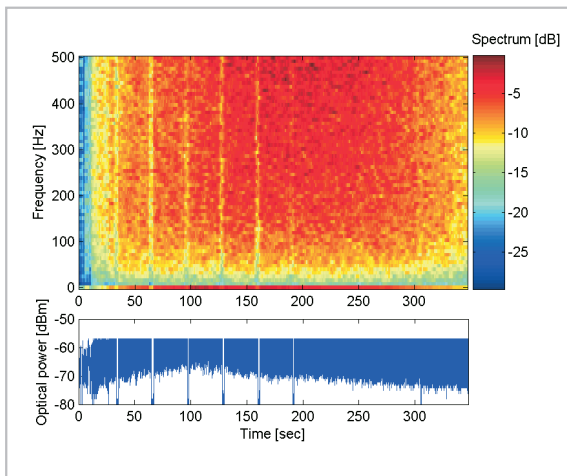
link power spectra were undersampled with a sampling frequency of 1 kHz due to the limited onboard data acquisition capability, which limited the frequency analysis to frequencies of up to 500 Hz. The dominant frequency spectra resided around several hundred hertz, and the frequency components were proportional to the elevation angle of the satellite as the satellite moved relatively faster at higher elevation angles than at lower elevation angles. Figure 27 shows the PSD of the downlink received power, indicating that frequency components existed up to about 1 kHz.

5.6 Communication performance

Figure 28 shows the bit error rate (BER) characteristics for an uplink. Each data point represents the BER for a data stream with a duration of 1 s. The power penalty for the up-

Fig.25 Long-term trends of the uplink received powers and the frequency spectra (March 28, 2006)
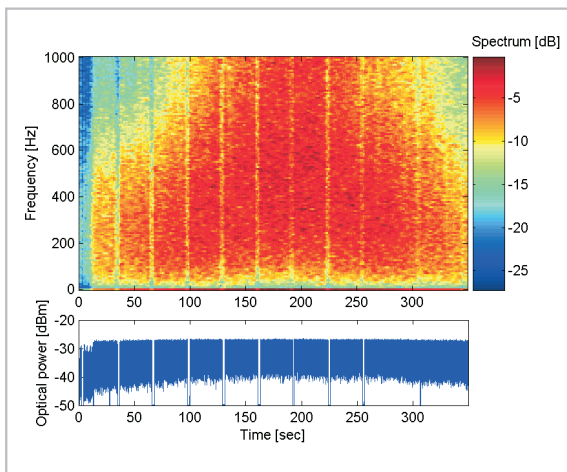
Fig.26 Long-term trends of the downlink received powers and the frequency spectra (March 28, 2006)
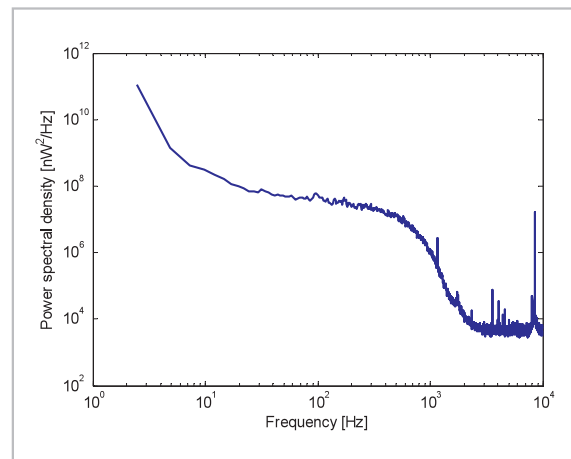

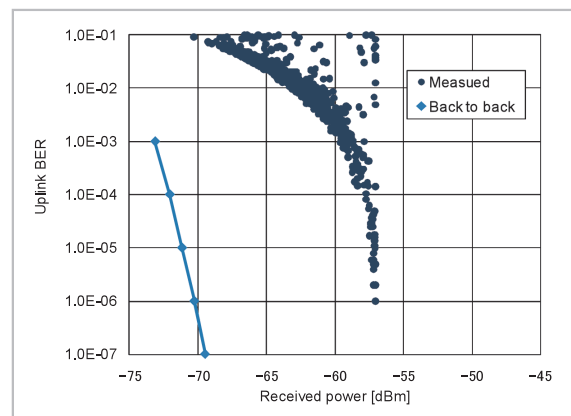**Fig.27** Power spectral density of the downlink received power (December 23, 2008)

Fig.28 Uplink BER (November 13, 2008)

link was –13 dB at a BER of 10^{-6} due to signal fluctuation induced by atmospheric turbulence. On the other hand, Fig. 29 shows the downlink BER results, where the power penalty for the

downlink was –13.5 dB at a BER of 10^{-5}. Each data point represents the BER for a data stream with duration of 1 s.
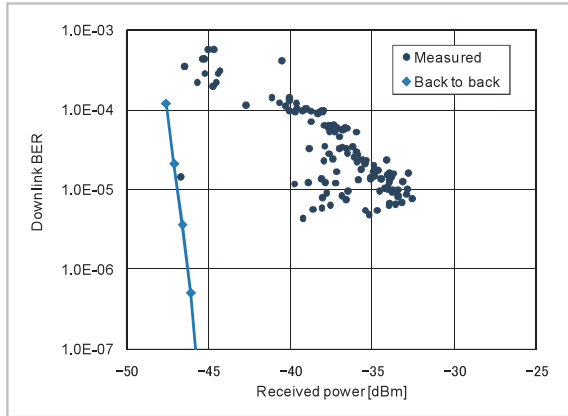
5.7 Link budget analysis

Table 4 shows an example of a link budget analysis for the experiment conducted on November 23, 2006. In this analysis, the laser beam propagation theory with a Gaussian beam was considered for the downlink [21]. Since a multimode fiber was used for the uplink, a plane wave was considered due to the uniform intensity pattern. Table 4 shows that the fade and surge levels for the uplink and downlink were smaller than the dynamic range of the sensors. Therefore, tracking was successfully maintained during the experiment. Here, the power penalties for the uplink and

Fig.29 *Downlink BER (November 13, 2008)*

Table 4 *Link budget analysis for the link between the NICT optical ground station and the OICETS satellite (November 13, 2008)*

Parameter	Unit	Uplink			Downlink	
		Beacon	Tracking	Comm.	Tracking	Comm.
TX power	W	3.76	0.36	0.36	0.10	0.10
	dBm	35.7	25.6	25.6	20.0	20.0
Beam diameter at telescope	cm	1.7	63.5	63.5	12.0	12.0
Pointing jitter	μrad (rms)	23.1	23.1	23.1	0.12	0.12
TX beam divergence	μrad	9000	167.7	167.7	9.0	9.0
TX optics loss	dB	–0.05	–18.5	–18.5	–2.7	–2.7
Wavelength	m	8.08E-07	8.15E-07	8.15E-07	8.47E-07	8.47E-07
Average pointing loss	dB	0.0	–0.3	–0.3	–2.3	–2.3
TX gain	dB	53.0	87.5	87.5	116.0	116.0
Distance	m	7.07E+05	7.07E+05	7.07E+05	7.07E+05	7.07E+05
Free space loss	dB	–260.8	–260.7	–260.7	–260.4	–260.4
Atmospheric transmission	dB	–1.3	–1.3	–1.3	–1.3	–1.3
RX antenna diameter	cm	26.0	26.0	26.0	31.8	31.8
RX gain	dB	120.1	120.0	120.0	121.4	121.4
RX optics loss	dB	–2.6	–7.6	–7.9	–19.9	–19.9
Tracking sensor power	dBm	–56.0	–55.3	–	–29.1	–
Fade level ($P_F = 10^{-2}$)	dB	–7.3	–3.4	–	–1.8	–
Surge level ($P_S = 10^{-2}$)	dB	5.5	3.0	–	1.6	–
Dynamic range	dB	12.8	6.4	–	3.4	–
RX power	dBm	–	–	–55.6	–	–29.1
Power penalty for average BER	dB	–	–	–13.0	–	–13.5
Data rate	bps	–	–	2.048E+06	–	4.937E+07
Sensitivity (at a BER of 10^{-6})	photons/bit	–	–	200	–	2200
	dBm	–	–	–70.0	–	–45.9
Average margin for BER	dB	–	–	**1.4**	–	**3.3**

downlink BERs were taken from Figs. 28 and 29, respectively, and the link margin was consistent for the measured uplink and downlink BERs. In the optical ground station system, only off-the-shelf commercial devices were used. However, the quality in terms of BERs measured in the experiment is sufficient for the use of commercial wireless communication links. In this regard, forward error correction (FEC) code, such as LDPC, can improve the BER. We tested the LDPC code, although the importance of using longer codes than those used in this experiment is well known. Based on these results, a novel communication protocol that is tolerant to fading has been developed [51], and it is expected to find application in the development of future optical communication link systems.

6 Measurement results for atmospheric turbulence

In the ground-to-satellite laser communication experiment, the laser beam propagation characteristics were first measured for the beam from the LEO satellite, and this section presents the results of measuring the level of atmospheric turbulence. The atmospheric turbulence model is developed on the basis of measured data and allows for examining the strength and time variation of signals in the presence of atmospheric turbulence. This section can be summarized as follows. In Subsection **6.1**, a modification is added to the conventional atmospheric turbulence theory on the basis of measurement results. Subsection **6.2** describes the measured experimental data, which shows a reduction in scintillation owing to aperture averaging. The scintillation index is shown in Subsection **6.3** as a function of the elevation angle of the satellite, where it decreases as the elevation angle increases. Furthermore, the results of measuring the seeing angle and the atmospheric coherence length are shown in Subsections **6.4** and **6.5**, respectively.

6.1 Modification of the atmospheric turbulence model for the NICT optical ground station

The seeing angle measured by using the DIMM method on September 19, 2006 is plotted in Fig. 30. The atmospheric coherence length and the seeing angle correspond to 4.96 cm and 4.75 arcsec respectively at an elevation angle of 35° toward OICETS. In Figure 30, the profile of the seeing angle becomes flat around the midpoint of the experiment, which is due to the first term in Eq. (1). Therefore, a new parameter M is introduced in Eq. (1) as follows

$$C_n^2(h) = M \times 0.00594(v/27)^2(10^{-5}h)^{10}\exp(-h/1000)$$
$$+ 2.7 \times 10^{-16}\exp(-h/1500) + A\exp(-h/100) \quad (1)$$

where M is the new parameter added for the NICT optical ground station and h is the altitude of the optical ground station. When C_n^2 becomes larger than 10^{-14}, the scintillation can be considered to be in the moderate-to-strong-turbulence regime. The rms wind speed v (m/s) is determined from

$$v = \left[\frac{1}{15 \times 10^3}\int_{5 \times 10^3}^{20 \times 10^3}V^2(h)dh\right]^{1/2} \quad (2)$$

where $V(h)$ is described by the Bufton wind model as

$$V(h) = \omega_g h + v_g + 30\exp\left(-\frac{h - 9400}{4800}\right) \quad (3)$$

Here, v_g is the ground wind speed and ω_g is the slew rate associated with satellite motion relative to an observer on the ground. The constants A and M in Eq. (1) were estimated to be
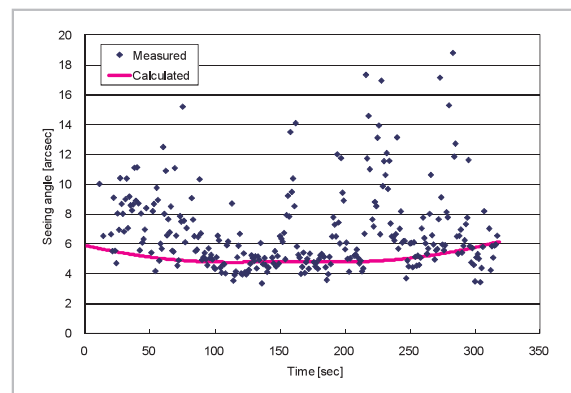

Fig.30 Seeing angles measured with the DIMM method on September 19, 2006, and calculated using the HV model

9.0×10^{-14} m$^{-2/3}$ and 0.2 at the optical ground station on the basis of DIMM measurements [52]. The structure parameter at the altitude of the optical ground station corresponds to C_n^2 (122 m) = 2.68×10^{-14} m$^{-2/3}$.

6.2 Comparison of scintillation indices

Figure 31 shows a comparison of the downlink scintillation indices measured by using photo detectors with different aperture sizes. The diameters of the three apertures used in the experiment were 1.5 cm, 5 cm, and 32 cm. The scintillation index with the 32-cm aperture was smaller than that with the 5-cm aperture due to the aperture averaging effect [49] [50]. On the other hand, the scintillation index obtained with the 1.5-cm aperture was much larger than the indices obtained with the other two apertures, and the variation was also large, which indicated that the atmospheric coherence length was smaller than 5 cm but larger than 1.5 cm in this experiment.

6.3 Scintillation index measurements

Figures 32 and 33 show the scintillation indices for the uplink and the downlink, respectively, as functions of the elevation angle of the satellite. The scintillation index decreases at higher elevation angles. For the uplink, the single beacon beam was received by the satellite only on March 21 and 28, and the scintillation index was large in value. With four laser beams, the scintillation index was
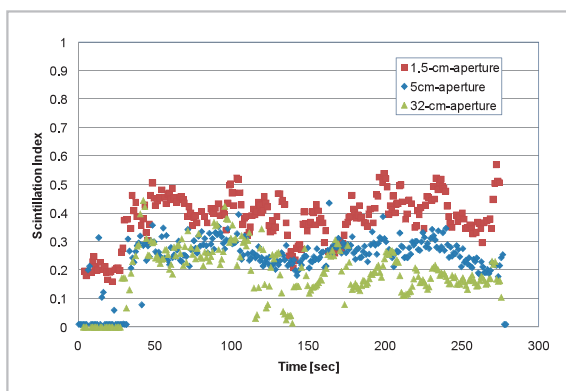
Fig.31 *Comparison of scintillation indices measured with different apertures (1.5 cm, 5 cm, and 32 cm in diameter) on November 20, 2009*

typically below 0.1 in the unsaturated data from September 19. For the downlink, the 20-cm telescope was used on March 21, 28, and 30, while the 31.8-cm sub-aperture in the 1.5-m telescope was used for the remaining days of the experiment. It is clear from Fig. 33 that the aperture averaging effect reduced the scintillation index. With the 31.8-cm sub-aperture, the index was typically below 0.2.

6.4 Seeing angle measurements

The seeing angle corresponds to the average angular spot size of stellar images in astronomy and is defined as the half-width of the fitted Gaussian distribution, which is a measure of the strength of atmospheric turbulence. The measured seeing angles are plotted in Figs. 34-36 on the basis of measurements with the DIMM method. The seeing angle can be converted into the atmospheric coherence length r_0. Figures 34 and 35 show the seeing angle as a function of the elevation angle with
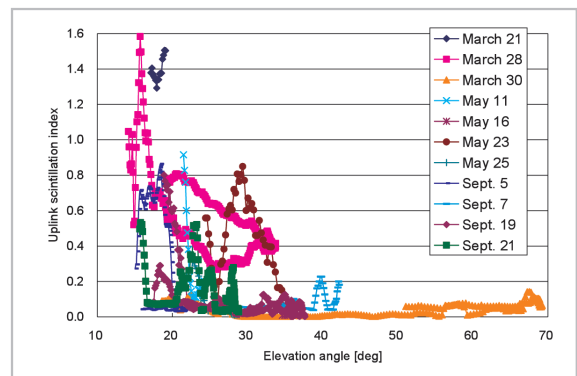
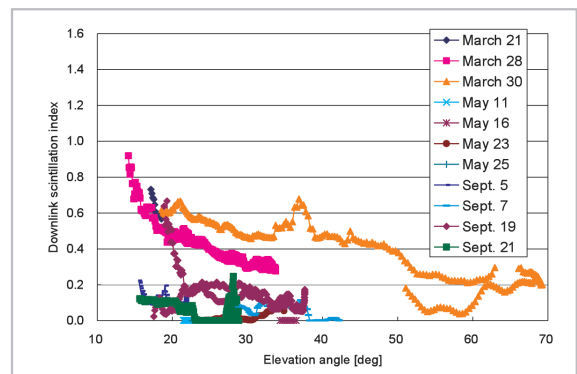**Fig.32** *Uplink scintillation index as a function of the elevation angle*

Fig.33 *Downlink scintillation index as a function of the elevation angle*
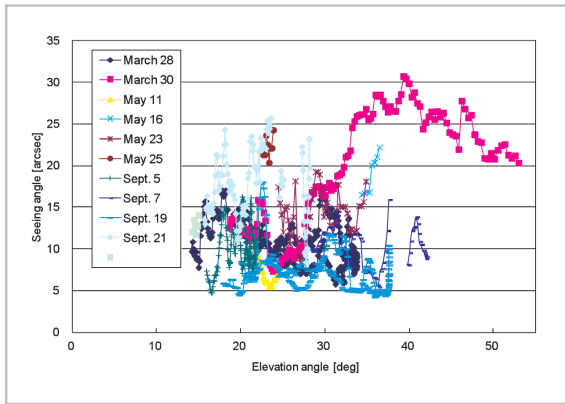
Fig.34 *Measured seeing angle as a function of the elevation angle of the satellite without zenith angle correction*
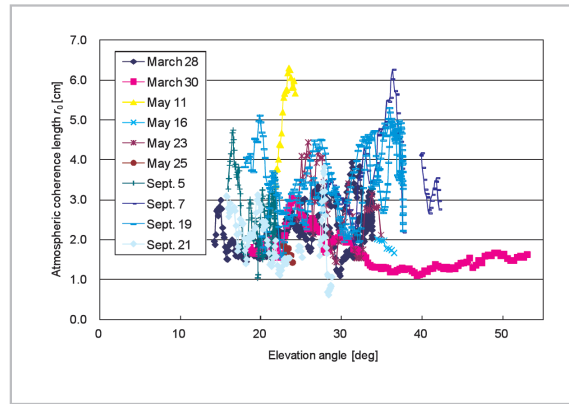

Fig.35 *Measured seeing angle as a function of the elevation angle of the satellite with zenith angle correction*

Fig.36 *Seeing angle as a function of angular velocity of satellite with zenith angle correction*

Fig.37 *Atmospheric coherence length as a function of the elevation angle of the satellite without zenith angle correction*
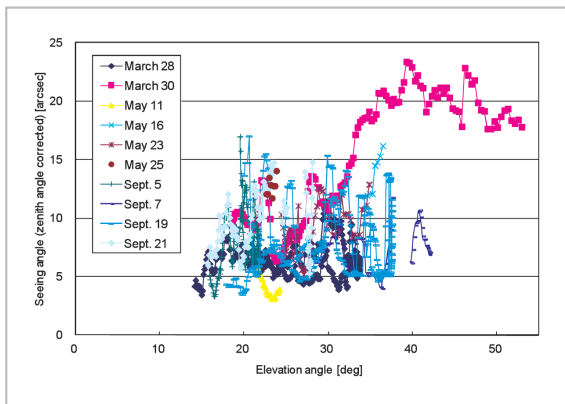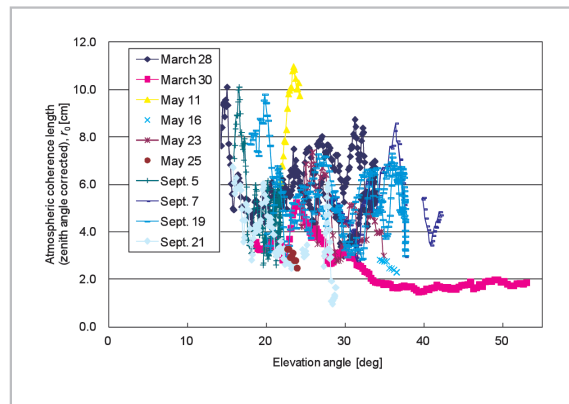

Fig.38 *Atmospheric coherence length as a function of the elevation angle of the satellite with zenith angle correction*
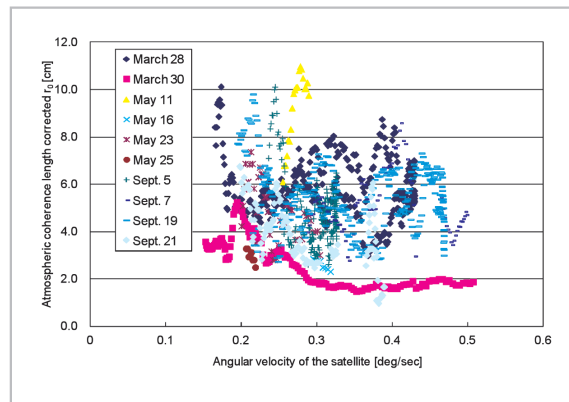
Fig.39 *Atmospheric coherence length as a function of the angular velocity of the satellite with zenith angle correction*

and without zenith angle correction, respectively. The zenith angle correction compensates for the difference in air mass at different elevation angles, and the seeing angles with the zenith angle correction were of the order of tenths of an arcsecond. Figure 36 shows the seeing angle as a function of the angular velocity of the satellite.

6.5 Atmospheric coherence length measurements

Similarly to Figs. 34–36, Figs. 37–39 show the measurement results for the atmospheric coherence length r_0 measured with the DIMM method. Figures 37 and 38 show the atmospheric coherence length as a function of the zenith angle with and without zenith angle correction, respectively. The atmospheric coherence length ranged between 1 and 6 cm in the experiments. Furthermore, Fig. 39 shows the atmospheric coherence length as a function of the angular velocity of the satellite.

7 Conclusion

Optical communication links between an LEO satellite and an optical ground station were successfully established, and the effects of atmospheric turbulence were simultaneously measured. Acquisition and tracking were successfully performed when clear-sky conditions prevailed, and optical links were successfully established even when there was atmospheric turbulence above the ground station.

Also, uplink scintillation was successfully reduced by using multiple laser beams, and downlink scintillation effectively decreased due to the aperture averaging effect. The uplink and downlink BER performance was evaluated with the measured power penalties, and the optical link budget was verified. Thus, this experiment served as an effective verification of the ability to establish ground-to-satellite laser communication links through the atmosphere. The results presented here are expected to contribute not only to the development of this scientific field, but also to the utilization and practical application of free-space laser communication in the future.

References

1   G. Hyde and B. Edelson, "Laser satellite communications: current status and directions," Space Policy, Vol. 13, pp. 47–54, 1997.

2   V. W. S. Chan, "Optical satellite networks," Journal of Lightwave Technology, Vol. 21, pp. 2811–2827, 2003.

3   M. Toyoshima, "Trends in satellite communications and the role of optical free-space communications [Invited]," Journal of Optical Networking, Vol. 4, pp. 300–311, 2005.

4   T. Jono, Y. Takayama, N. Kura, K. Ohinata, Y. Koyama, K. Shiratama, Z. Sodnik, B. Demelenne, A. Bird, and K. Arai, "OICETS on-orbit laser communication experiments (Invited Paper)," Proc. SPIE, Vol. 6105, pp. 13–23, 2006.

5   M. Toyoshima, T. Takahashi, K. Suzuki, S. Kimura, K. Takizawa, T. Kuri, W. Klaus, M. Toyoda, H. Kunimori, T. Jono, Y. Takayama, and K. Arai, "Results from Phase-1, Phase-2 and Phase-3 Kirari Optical Communication Demonstration Experiments with the NICT optical ground station (KODEN)," 24th International Communications Satellite Systems Conference of AIAA, AIAA-2007-3228, Korea, April 13, 2007.

6   T. Abe, T. Kizaki, H. Kunimori, Y. Takayama, and M. Toyoshima, "The development of two-axes fast steering mirror and high efficiency driver," International Conference on Space Optical Systems and Applications 2009 (ICSOS2009), ICSOS2009-30, Feb. 2009.

7   Y. Kadoike, E. Okamoto, Y. Iwanami, Y. Shoji, M. Toyoshima, Y. Takayama, and H. Kunimori, "LDPC code design for OICETS experiments in 2008," International Conference on Space Optical Systems and Applications 2009 (ICSOS2009), ICSOS2009-41, Feb. 2009.

8 T. Tanaka, M. Abe, M. Morimoto, Y. Kadoike, E. Okamoto, Y. Shoji, and M. Toyoshima, "Development of LDPC codes by the Gallager composition method on FPGA," International Conference on Space Optical Systems and Applications 2009 (ICSOS2009), ICSOS2009-29, Feb. 2009.

9 A. N. Kolmogorov, "The local structure of turbulence in an incompressible viscous fluid for very large Reynolds numbers," C. R. (Doki) Acad. Sci. U.S.S.R., Vol. 30, pp. 301–305, 1941.

10 V. I. Tatarskii, "The Effect of the Turbulent Atmosphere on Wave Propagation", Trans. for NOAA by Israel program for scientific translations, Jerusalem, 1971.

11 D. L. Fried, "Scintillation of a ground-to-space laser illuminator," J. Opt. Soc. Am., Vol. 57, No. 8, pp. 980–983, 1967.

12 P. O. Minott, "Scintillation in an earth-to-space propagation path," J. Opt. Soc. Am., Vol. 62, No. 7, pp. 885–888, 1972.

13 P. J. Titterton, "Scintillation and transmitter-aperture averaging over vertical paths," J. Opt. Soc. Am., Vol. 63, No. 4, pp. 439–444, 1973.

14 P. J. Titterton, "Power reduction and fluctuations caused by narrow laser beam motion in the far field," Appl. Opt., Vol. 12, No. 2, pp. 423–425, 1973.

15 D. L. Fried, "Statistics of laser beam fade induced by pointing jitter," Appl. Opt., Vol. 12, No. 2, pp. 422–423, 1973.

16 J. L. Bufton, "Scintillation statistics measured in an earth-space-earth retroreflected link," Appl. Opt., Vol. 16, No. 10, pp. 2654–2660, 1977.

17 H. T. Yura and W. G. McKinley, "Optical scintillation statistics for IR ground-to-space laser communication systems," Appl. Opt., Vol. 22, No. 21, pp. 3353–3358, 1983.

18 P. A. Lightsey, "Scintillation in ground-to-space and retroreflected laser beams," Opt. Eng., Vol. 33, No. 8, pp.2535–2543, 1994.

19 K. Kiasaleh, "On the probability density function of signal intensity in free-space optical communications systems impaired by pointing jitter and turbulence," Opt. Eng., Vol. 33, No. 11, pp. 3748–3757, 1994.

20 J. D. Shelton, "Turbulence-induced scintillation on Gaussian-beam waves: theoretical predictions and observations from a laser-illuminated satellite," J. Opt. Soc. Am. A, Vol. 12, No. 10, pp. 2172–2181, 1995.

21 L. C. Andrews, R. L. Phillips, and P. T. Yu, "Optical scintillations and fade statistics for a satellite-communication system," Appl. Opt. Vol. 34, No. 33, pp. 7742–7751, 1995. Errata: Vol. 36, No. 24, p. 6068, 1997.

22 R. J. Hill and R. G. Frehlich, "Probability distribution of irradiance for the onset of strong scintillation," J. Opt. Soc. Am A, Vol. 14, No. 7, pp. 1530–1540, 1997.

23 L. C. Andrews, R. L. Phillips, C. Y. Hopen, and M. A. Al-Habash, "Theory of optical scintillation," J. Opt. Soc. Am. A, Vol. 16, No. 6, pp. 1417–1429, 1999.

24 L. C. Andrews, R. L. Phillips, and C. Y. Hopen, "Scintillation model for a satellite communication link at large zenith angles," Opt. Eng., Vol. 39, No. 12, pp. 3272–3280, 2000.

25 Y. Furuhama, Y. Masuda, T. Shinozuka, and M. Fukushima, "Propagation Characteristics of Laser Wave Through the Turbulent Atmosphere-Cumulative Probability Distribution," Journal of the IEICE, Vol. 56-B, No. 4, pp. 133–139, 1973.

26 K. Funakawa, "Atmospheric propagation of laser waves," IEICE, Vol. 51, No. 4, pp. 503–510, April, 1968.

27 T. Aruga, K. Araki, T. Igarashi, F. Imai, Y. Yamamoto, and F. Sakagami, "Earth to space laser beam transmission for spacecraft attitude measurement," Applied Optics, Vol. 23, pp. 114–147, 1984.

28 T. Aruga, K. Araki, R. Hayashi, T. Iwabuchi, M. Takahashi, and S. Nakamura, "Earth-to-geosynchronous satellite laser beam transmission," Applied Optics, Vol. 24, No. 1, pp. 53–56, 1985.

29 K. Araki, T. Itabe, M. Takabe, T. Aruga, and H. Inomata, "Experiments on CO2 Laser Beam Transmission from Ground to Geostationary Meteorological Satellite-III," Laser Sensing Simposium, C4, pp. 47–48, May, 1988.

30   M. Takabe, K. Araki, M. Toyoda, T. Itabe, and T. Aruga, "Application of Optical Beacon for Earth Image Calibration," Journal of the Remote Sensing Society of Japan, Vol. 13, No. 2, pp. 53–60, 1993.

31 T. Aruga, T. Itabe, M. Ishizu, M. Takabe, N. Hiromoto, and M. Shikatani, "A new optical facility for multi-purpose studies," Denshi Tokyo, Vol. 27, pp. 53–56, 1988.

32 H. Kunimori, K. Imamura, F. Takahashi, T. Itabe, T. Aruga, and A. Yamamoto, "New development of satellite laser ranging system for highly precise space and time measurements," J. Comm. Res. Lab., Vol. 38, No. 2, pp. 303–317, 1991.

33 N. Koga, N. Sugimoto, K. Ozawa, Y. Saito, A. Nomura, A. Minato, T. Aoki, T. Itabe, and H. Kunimori, "Laser long-path absorption experiment using the Retroreflector in Space (RIS) on the ADEOS satellite," Proc. SPIE, Vol. 3218, pp. 10–18, 1997.

34 H. Kunimori, S. Oya, and Y. Nakamura, "Optical tracking and ranging to a satellite in GTO by 1.5 m telescope," Proceedings of CRL International Symposium on Light Propagation and Sensing Technologies for future applications, March 13–14, Tokyo, pp. 97–98, 2002.

35 H. Kunimori et.al, "Integration of 1.5 m Telescope and Ranging System in CRL," 13th International Workshop on Laser Ranging, Washington, DC., USA, Oct. 7–11, 2002.

36 Y. Arimoto, H. Okazawa, M. Shikatani, T. Takahashi, M. Toyoda, M. Toyoshima, and K. Araki, "Laser communication experiment using ETS-VI satellite," CRL Journal, Vol. 42, No. 3, pp. 285–292, Nov. 1995.

37 K. E. Wilson, J. R. Lesh, K. Araki, and Y. Arimoto, "Overview of the Ground-to-Orbit Lasercom Demonstration," Space Communications, Vol. 15, pp. 89–95, 1998.

38 S. Kimura, H. Yamamoto, Y. Nagai, S. Nakasuka, H. Hashimoto, and S. Nishida, "In-orbit Demonstration of Orbital Maintenance System Using COTS Technologies," Annual conference of IEICE 2004, SB-8-4, pp. SE-11~SE-12, March, 2004.

39 M. Toyoshima, H. Kunimori, Y. Takayama, S. Kimura, Y. Nagai, H. Yamamoto, H. Hashimoto, N. Takahashi, M. Kato, and T. Yamamoto, "Ground-to-Orbit Laser transmission Experiments with MicroLabSat (GOLEM)," Technical Report of IEICE, Proc. SANE2004-45(2004-8), Vol. 104, No. 271, pp. 17–22, 2004.

40 M. Toyoshima, H. Takenaka, Y. Shoji, Y. Takayama, Y. Koyama, and M. Akioka, "Small Optical Transponder for Small Satellites," International Symposium on Communication Systems, Networks and Digital Signal Processing, 2nd Colloquium in Optical Wireless Communications at the IEEE International Conference (CSND-SP10), OWC-10, Northumbria University, United Kingdom, July 21–23, 2010.

41 M. Reyes, S. Chueca, A. Alonso, T. Viera, and Z. Sodnik, "Analysis of the preliminary optical links between ARTEMIS and the Optical Ground Station," Proc. SPIE, Vol. 4821, pp. 33–43, 2003.

42 P. A. Lightsey, "Scintillation in ground-to-space and retroreflected laser beams," Opt. Eng., Vol. 33, No. 8, pp. 2535–2543, 1994.

43 I. I. Kim, B. Riley, N. M. Wong, M. Mitchell, W. Brown, H. Hakakha, P. Adhikari, and E. J. Korevaar, "Lessons learned for STRV-2 satellite-to-ground lasercom experiment," Proc. SPIE 4272, 1–15, 2001.

44 I. I. Kim, H. Hakakha, P. Adhikari, E. Korevaar, and A. K. Majumdar, "Scintillation reduction using multiple transmitters," Proc. SPIE, Vol. 2990, pp. 102–113, 1997.

45 R. K. Tyson, "Adaptive optics and ground-to-space laser communications," Applied Optics, Vol. 35, No. 19, pp. 3640–3646, 1996.

46 M. Toyoshima and K. Araki, Japan Patent Application for a "Beam splitting method," No. 3069703, filed 24 Nov. 1999.

47 M. Sarazin and F. Roddier, "The ESO differential image motion monitor," Astron. Astrophys. 277, 294–300, 1990.

48 Y. Takayama, T. Jono, M. Toyoshima, H. Kunimori, D. Giggenbach, N. Perlot, K. Shiratama, J. Abe, and K. Arai, "Tracking and pointing characteristics of OICETS optical terminal in communication demonstrations with ground stations (Invited)," Proc. SPIE 6457A, 6457A-07, 2007.

49 L. C. Andrews and R. L. Phillips, "Laser Beam Propagation through Random Media," SPIE Optical Engineering Press, Bellingham, Wash., Second edition, 2005.

50 D. L. Fried, "Aperture averaging of scintillation," J. Opt. Soc. Am. 57(2), 169–175, 1967.

51 J. H. Churnside, "Aperture averaging of optical scintillations in the turbulent atmosphere," Appl. Opt. 30(15), 1982–1994, 1991.

52 Y. Suzuki, Y. Koishi, Y. Hasegawa, Y. Hashimoto, S. Murata, T. Yamashita, K. Shiratama, M. Toyoshima, and Y. Takayama, "Optical Free Space Communication System for 40Gbps Data Downlink from Satellite/Airplane," Proc. AIAA ICSSC 2011, Nara, Nov. 29, 2011.

53 M. Toyoshima, Y. Takayama, H. Kunimori, S. Yamakawa, and T. Jono, "Characteristics of laser beam propagation through the turbulent atmosphere in ground-to-low earth orbit satellite laser communications links," IEICE Trans. on Communications J94-B, 3, 409–418, 2011.

TOYOSHIMA Morio, *Ph.D.*

Director, Space Communication Systems Laboratory, Wireless Network Research Institute

Satellite Communications, Atmospheric Turbulence, Laser Communications, Quantum Cryptography

KLAUS Werner, *Ph.D.*

Senior Researcher, Photonic Network System Laboratory, Photonic Network Research Institute

Free-space laser communications, Microoptics, Diffractive Optics, Electromagnetic Field Analysis, Fiber Optics

TAKENAKA Hideki

Limited Term Technical Expert, Space Communication Systems Laboratory, Wireless Network Research Institute

Satellite Communications, Laser Communications

TAKAYAMA Yoshihisa, *Dr. Eng.*

Senior Researcher, Space Communication Systems Laboratory, Wireless Network Research Institute

Nonlinear Optics, Phase Conjugate Optics, Photonic Crystals, Computational Electromagnetics, Space Laser Communications

KUNIMORI Hiroo

Senior Researcher, Space Communication Systems Laboratory, Wireless Network Research Institute

Satellite Laser Ranging

YAMAKAWA Shiro, *Ph.D.*

Senior Engineer, Space Applications Mission Directorate, Space Applications Program Systems Engineering Office, Satellite Systems Engineering Group, Japan Aerospace Exploration Agency (JAXA)

Satellite System, Satellite Communications, Space Optical Communication

KURI Toshiaki, *Ph.D.*

Director, Planning Office, Photonic Network Research Institute

Optical Communication Systems, Radio-over-Fiber

TOYODA Masahiro

Research Promotion Expert, Information Systems Office, Outcome Promotion Department

Wave Propagation in Turbulent Media

SHOJI Yozo, *Ph.D.*

Planning Manager, New Generation Network Laboratory, Network Research Headquarters

Millimeter-wave Communications System, Microwave-Photonics Systems, Coherent Laser Communications System, Wired & Wireless Network Virtualization

KOYAMA Yoshisada

Expert Researcher, Space Communication Systems Laboratory, Wireless Network Research Institute

Optical Communications, Onboard Equipment

JONO Takashi

Associate Senior Engineer, Tokyo Office, Japan Aerospace Exploration Agency (JAXA)

Satellite System, Satellite Communication

ARAI Katsuyoshi

Director, Ground Facilities Department, Japan Aerospace Exploration Agency

Spacecraft Development Project (BSE, BS-2, MDS-1, OICETS), JEM Development Project